A.S. Marfunin (Ed.)

Advanced Mineralogy

Volume 2
Methods and Instrumentations: Results and Recent Developments

With 120 Figures and 18 Tables

Springer-Verlag
Berlin Heidelberg New York
London Paris Tokyo
Hong Kong Barcelona
Budapest

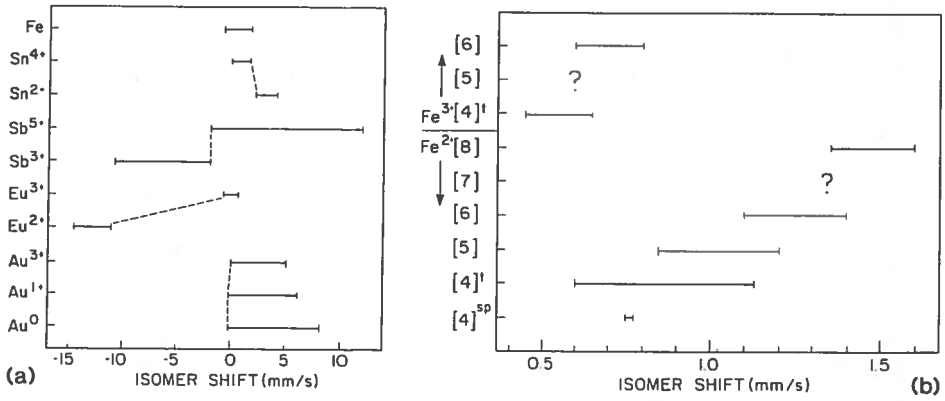

Fig. 24a,b. Isomer shift ranges for selected isotopes in various valence states: ^{57}Fe relative to Fe-foil, ^{119}Sn relative to SnO_2, ^{121}Sb relative to InSb, ^{151}Eu relative to Eu_2O_3, ^{197}Au relative to pure ^{197}Au. **a** All isotopes, note the wide range for species whose valence changes involve s-electrons (with the exception of ^{197}Au). **b** Results for ^{57}Fe, showing the effect of coordination number and valence. (After Hawthorne 1988)

applied magnetic field, or it can be intrinsic and due to unpaired orbital electrons. Thus Mössbauer spectroscopy is an important tool in the study of the magnetic properties of minerals.

Determination of Site Occupancies

The most common application of Mössbauer spectroscopy in mineralogy involves the determination of ^{57}Fe site-occupancies in minerals. In a mineral, for each crystallographically unique site partly occupied by Fe in either valence state, there will be a quadrupole-split doublet. Assuming that the recoil-free fraction of Fe is the same at each site, the relative intensities of the doublets give the relative amounts of Fe (Fe^{2+} and Fe^{3+}) at the different sites, provided the total Fe content of the mineral is known from a chemical analysis. Such results play a significant role in thermodynamic modeling of minerals.

3.1.2 Experimental Techniques and Spectrum Fitting

F.C. Hawthorne, A.V. Bykov, N.N. Delyagin, and V.I. Nikolaev

The experimental set-up of a Mössbauer spectrometer is fairly simple; a scheme is shown in Fig. 25a. A radioactive γ-ray source is attached to a vibration mechanism (drive) that imparts a Doppler shift to the emitted γ-ray energy. The modulated γ-ray passes through the sample where that component with the

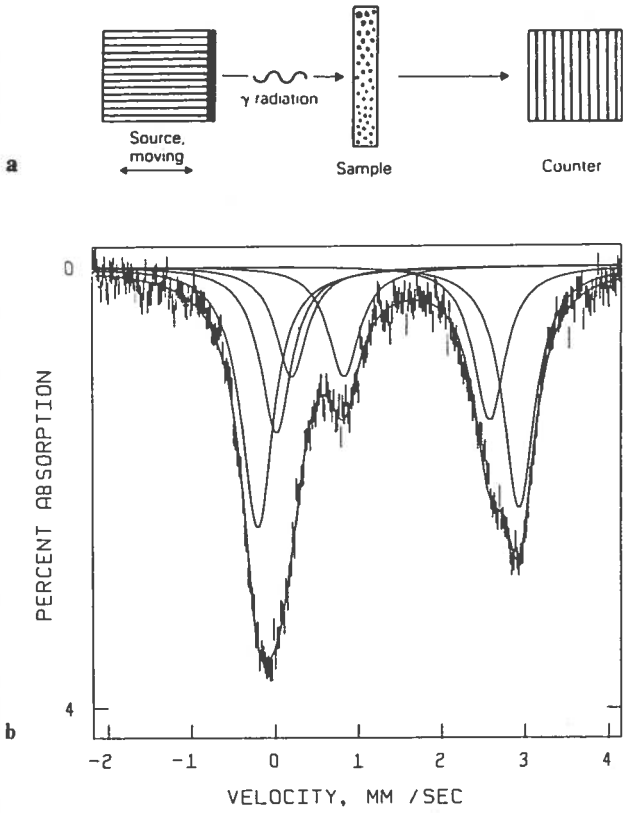

Fig. 25a, b. Scheme of an experimental arrangement for transmission Mössbauer spectroscopy. **b** An experimental Mössbauer spectrum; the data are represented by *vertical dashes*, the length of which represents $\pm \sigma$ based on counting statistics, the individual doublets are the fitted components of the spectrum, and the *line through the data points* is the envelope of the fitted spectrum. (After Hawthorne 1988)

appropriate energy is absorbed. The γ-ray then passes into a detector and the resulting signals are accumulated (as a function of source velocity) in a multichannel analyzer (MCA); this is the raw spectrum.

Drive Mechanism

The drive transmits a constant acceleration (alternately positive and negative) to the source such that a range of velocities is scanned linearly and repeatedly. The energy of the resultant γ-ray at any instant is related to the velocity of the source, and the spectrum is recorded in terms of γ-ray intensity as a function of source velocity. The vibration of the source is driven by a sawtooth waveform of a symmetric (⋀⋀) or asymmetric (◿◸) form. In the symmetric form (which is

more common), the source moves towards the sample with a constant acceleration while the MCA accumulates counts over half the channels, and then the source moves away from the sample while the MCA accumulates counts over the other half of the channels. This generates mirror image spectra in each half of the MCA; during processing, this double spectrum is folded back upon itself to give a single spectrum of the sample. In the asymmetric form, a single spectrum is accumulated over most ($> 95\%$) of the channels in the MCA; this waveform is more difficult to generate reproducibly.

Detectors

For ^{57}Fe, good resolution can be obtained with a scintillation counter or a proportional counter; a proportional counter is more commonly used, usually positioned such that it senses the transmitted γ-rays (Fig. 25a).

Sample Preparation

For most applications, powdered samples are used. The sample must be of uniform thickness and the grains of the powder must be randomly oriented. An inert matrix can help alleviate problems of preferred orientation. Ideally, it should be inert, granular, softer than the sample, iron-free and easy to remove (preferable soluble, e.g., sugar, salt); graphite is often used for high-temperature spectroscopy.

The theoretical arguments concerning derivation of site-occupancies from peak intensities are generally developed for infinitely thin absorbers. Excessive γ-ray absorption leads to peak-shape degradation, a nonlinear baseline, peak broadening, and saturation effects. For many years, there has been a general rule that for Fe-bearing minerals, an Fe content of ~ 5 mg/cm^2 is a good compromise between a thin absorber and good counting statistics. However, thickness corrections are necessary for very accurate work; these are applied by running the spectra at various sample thicknesses and extrapolating the results to an infinitely thin sample.

Calibration

In the experiment, the peak positions are measured not in terms of their true energies but in relation to a zero energy point and an energy scale derived from a standard absorber spectrum. For absorbers of mineralogical interest, the following standards are commonly used: ^{57}Fe: iron foil, stainless steel, sodium nitroprusside; ^{119}Sn: SnO_2; ^{121}Sb: InSb. For ^{57}Fe, the relative conversion factors are: stainless steel: 0.10 mm/s; sodium nitropruside: 0.257 mm/s.

Spectrum Quality

The variance of the counts in a specific channel of the MCA is equal to the number of counts. Hence, assuming only random error, the relative precision can be increased by counting for longer times, but this improvement tails off with increasing time. The optimum baseline (off-resonance) count is of the order of $1–5 \times 10^6$ counts/channel, usually taking 24–48 h for ^{57}Fe in most minerals, and providing an acceptable balance between the need for precision and the desire for experimental efficiency.

The Mössbauer Spectrum

An experimental spectrum is shown in Fig. 25b. Each vertical dash represents the number of counts recorded in that specific channel (source-velocity interval) together with its associated standard deviation based on counting statistics. The counts at the edges of the spectrum (zero absorption) are the intensity of the γ-ray beam over those energy ranges where no absorption has occurred. Towards the center of the spectrum, the counts decrease due to resonant absorption of γ-rays by the sample. The ideal line shape is *Lorentzian* (see below), and an observed spectrum ideally consists of a series of Lorentzian lines, the number and characteristics of which are a function of the Mössbauer nucleus and the crystal structure of the sample. There is often complex overlap of individual lines, and the derivation of quantitative information (peak position, widths, and areas) from such spectra requires numerical spectrum fitting.

A Mathematical Description

The ideal shape of a peak is Lorentzian. However, there are a number of factors that can result in a *Gaussian* component in the peak shape. Thus the description of the peak shape can be represented as a combination of these two forms (other more complex functions are also possible). This being the case, the intensity of the γ-radiation transmitted by the sample as a function of its energy, x, can be written as

$$y = b - \sum_{i=1}^{l}\left[\frac{(1-\alpha)2A_i/\pi\Gamma_i}{1+4(x-x_i)^2/\Gamma_i^2} + \frac{\alpha 2A_i}{\Gamma_i} - \sqrt{\frac{\ln 2}{\Gamma_i}}\exp\left\{-4\ln 2\left(\frac{x-x_i}{\Gamma_i}\right)^2\right\}\right],$$

where l is the number of lines, b is the background intensity, α is the fractional Gaussian character of the line, A_i is the area (intensity) of the ith line, Γ_i is the half-width of the ith line, x_i is the position of the ith line, y is the channel count, and x is the channel number.

Slight linear and sinusoidal deviations can occur in the background intensity due to source movement and instrumental drift; this can be incorporated by writing the background intensity, b, as a function of channel number:

$$b = b_0 + b_1 x + b_2 \sin(\pi x/w),$$

where b_j are refinable parameters and w is the width of the spectrum in channel numbers. More complex background models are possible.

Spectrum Fitting

The equations for the spectrum given above are not linear in all variables, and they must be linearized via some expansion approximation. The variable parameters of the equation are then adjusted by *least-squares refinement* in order to achieve agreement between the calculated spectrum and the observed spectrum. As the initial equations of the spectral model are not linear, the process has to be iterated, gradually approaching the optimum values for which there is a good fit between the equation of the envelope and the observed data (Fig. 25b).

When there is significant peak overlap in the spectrum, as in Fig. 25b, the refinement procedure is more difficult as the variables can now interact with one another in the refinement procedure. In this case, the spectrum inherently contains less information than is the case when there is no peak overlap. As a consequence of this, the precision of the calculated parameters is less due to significant correlation in the fitting procedure; in these circumstances, it is of crucial importance that all variable be refined simultaneously in the final cycle of refinement, and that the full variance-covariance matrix be used in the calculation of the standard deviations. Linear constraints can be used in the fitting process to reduce correlation between variable parameters. However, it is important that such constraints be correct, or else the precision will be improved but the accuracy will be degraded.

Goodness-of-Fit Criteria

The least-squares method minimizes the weighted sum of the squares between the observed and "calculated" data:

$$\chi_0^2 = \sum_{i=1}^{N} \frac{1}{\sigma_i^2}[y_i - f(x_i)]^2,$$

where y_i is the observed count in the ith channel, σ_i is the weight assigned to the ith observation, $f(x_i)$ is the calculated count in the ith channel, and N is the number of channels.

We may define the ideal residual χ_I^2 as

$$\chi_I^2 = \sum_{i=1}^{n} \frac{1}{\sigma_i^2}[y_i - f_I(x_i)]$$

where $f_I(x)$ is the true function. χ_I^2 follows the chi-squared distribution, and χ_0^2 is a value from this distribution if the parameters of the fitted function f(x) are a valid approximation to the true function $f_I(x)$. To test whether this is the case, one uses the distribution to assess the probability that $R_0 < R_i$ at a certain percentage confidence limit. At the 1% point on the chi-squared distribution, there is a 1% probability that χ_I^2 will exceed this value. Thus if $\chi_0^2 > 1\%$ point, then f(x) is generally accepted as a good approximation to $f_I(x)$ and the "fit" is acceptable. Within the 1% and 99% points of the chi-squared distribution, there is no statistical justification for preferring a fit with a lower χ_0^2 value as the probability that χ_I^2 will exceed χ_0^2 is quite high within these limits. There are other statistical indicators (reduced χ^2, MISFIT) that are also used as goodness-of-fit parameters.

Statistical acceptability is no guarantee that the derived model is correct; it merely indicates that the model adequately (but not exclusively) explains the observed data. One must judge whether or not the observed model is correct on the basis of whether or not it is physically and chemically reasonable.

3.1.3 Iron-Containing Minerals, Ores and Glasses

G. Amthauer, F.C. Hawthorne, and E. Polshin

There has been a large amount of work on iron-bearing minerals, focusing primarily on the derivation of site occupancies and oxidation ratios. We will first survey some site-occupancy results on important rock-forming minerals, and then go on to examine the use of Mössbauer spectroscopy in characterizing next-nearest-neighbor effects, structural phase transitions, and magnetic properties.

Garnets

There are three cation sites in the garnet structure: {X} (dodecahedral), [Y] (octahedral) and (Z) (tetrahedral); all of these can be occupied by Fe in one or more valence states, and Fig. 26 shows some resultant spectra. In the derivation of site-occupancies, it is usually assumed that the recoil-free fractions in the sample are the same at each non-equivalent site in the structure. The recoil-free fraction is related to the mean-squared vibrational displacement of the Mössbauer nucleus. Crystal structure refinements of garnets show that the mean-squared vibrational displacement of atoms at the {X}, [Y], and (Z) sites are distinctly different (being related to coordination number and mean bond-valence). Thus there should be significant differences in recoil-free fractions at the three sites in garnet. Mössbauer spectra of garnets recorded at different temperatures show that this is indeed the case. There is a strong differential